

Novel Self-Supported Natural and Synthetic Polymer Membranes for Air Humidification

S.D. Bhat,¹ A. Manokaran,¹ A.K. Sahu,¹ S. Pitchumani,¹ P. Sridhar,¹ A.K. Shukla^{1,2}

¹Central Electrochemical Research Institute, Karaikudi 630 006, India

²Solid State and Structural Chemistry Unit, Indian Institute of Science, Bangalore 560 012, India

Received 3 April 2008; accepted 16 February 2009

DOI 10.1002/app.30260

Published online 28 April 2009 in Wiley InterScience (www.interscience.wiley.com).

ABSTRACT: Novel self-supported natural and synthetic polymer membranes of chitosan-hydroxy ethyl cellulose-montmorillonite (CS-HEC-MMT) and polyvinyl alcohol (PVA)-polystyrene sulfonic acid (PSSA) are prepared by solution casting method followed by crosslinking. These membranes are employed for air humidification at varying temperatures between 30°C and 70°C and their performances are compared with commercial Nafion[®] membranes. High water fluxes with desired humidified-air output have been achieved for CS-HEC-MMT and PVA-PSSA hybrid membranes at air-flow rates of 1–10 slpm. Variation in the

air/water mixing ratio, dew point, and relative humidity that ultimately results in desired water flux with respect to air-flow rates are also quantified for all the membranes. Water flux values for CS-HEC-MMT are less than those for Nafion[®] and PVA-PSSA membranes, but the operational stability of CS-HEC-MMT membrane is higher than PVA-PSSA and comparable with Nafion[®] both of which can operate up to 70°C at repetitive cycles of humidification. © 2009 Wiley Periodicals, Inc. *J Appl Polym Sci* 113: 2605–2612, 2009

Key words: water flux; hybrid membrane; sorption; PEFC

INTRODUCTION

Water management is vital to the successful operation of polymer electrolyte fuel cells (PEFCs).^{1–4} It is well established that water management in PEFCs is related to the hydration level of the polymer electrolyte membrane, which is generally achieved by humidifying the reactant gases.^{5–8} There are two ways for humidifying reactant gases in PEFCs, namely external and internal humidification. Most of the external humidifiers are bubble humidifiers wherein reactant gas feeds are humidified by passing water vapor into the dry air. In the internal humidification, product water from the PEFC is used to humidify the reactant gases. In such a humidifier, liquid water from the PEFC and dry air from an external source are fed to either side of the membrane humidifier creating a water activity gradient across the membrane thereby forcing the water to diffuse through the membrane from the water side to the air side that subsequently evaporates at the membrane/air interface humidifying the air.^{9,10}

Humidification system using water permeable polymeric membranes are documented to be effective in humidifying reactant gases supplied to the

fuel cells.^{11,12} In any membrane humidifier, it is desirable that the membrane should be water permeable and should resist transmission of reactant gases or other components.^{13–15} To this end, different types of membranes, namely Nafion[®], cellophane, and other ultrafiltration membranes such as polysulfone and reverse osmosis membranes like polyamide and its derivatives have been used for humidifying the PEFCs.^{16,17} However, the limitations of these membranes are their high cost, large pore size, and gas permeability within and across the membrane. It is noteworthy that these membranes were originally designed for a specific purpose and later exploited for humidification.

In this communication, to obviate the aforesaid limitations, novel alternative cost-effective self-supported membranes, especially suitable for humidification of PEFCs, are reported. Self-supported hybrid polymeric membranes adopt the principle of pervaporation, wherein sorption of water molecules takes place at the interface of the membrane followed by diffusion across the membrane due to concentration gradient (rate-determining step) and desorption into vapor phase.^{18,19} These steps help realizing higher water flux during the humidification process. Such a situation also provides the possibility to custom-design membranes to satisfy the above characteristics. Accordingly, the choice for identifying new hybrid polymers that offer higher flux and selectivity to water depends on the appropriate selection of

Correspondence to: A.K.Shukla (shukla@sscu.iisc.ernet.in).
Contract grant sponsor: CSIR, New Delhi.

polymeric materials for producing membranes for humidification. The present study describes the use of two novel polymer hybrids, namely polymers comprising chitosan (CS)-hydroxy ethyl cellulose (HEC) with montmorillonite (MMT) as an inorganic filler and polymers comprising polyvinyl alcohol (PVA) and polystyrene sulfonic acid (PSSA) for membrane humidification. The results obtained are compared with widely used commercial Nafion[®] membranes.

EXPERIMENTAL

Materials

CS, HEC, and PVA were procured from Loba Chemicals, Mumbai (India). Montmorillonite and poly (sodium-*p*-styrene sulfonate) were obtained from Acros Chemicals (USA). Nafion[®] membranes were procured from Dupont (USA) and injection-molded graphite plates were obtained from Schunk (Germany). Deionized water (18.4 M Ω cm) from a Millipore system was used in the study.

Membrane preparation

Natural polymer hybrids were prepared as follows. A 100 mL of CS and HEC were dissolved separately in 10 wt % acetic acid to form clear solutions and were mixed under mechanical stirring in several proportions, more preferably as 75 CS : 25 HEC. Subsequently, 5 wt % of MMT in 10 wt % acetic acid solution was ultrasonicated for about 5 h followed by addition to CS : HEC solution to form a polymeric hybrid. The solution was further stirred for 24 h and casted as a membrane on a smooth flat Plexiglas plate at ambient temperature ($\sim 30^{\circ}\text{C}$). The hybrid membrane thus produced was externally crosslinked with 3 wt % H₂SO₄ in aqueous acetone mixture in a bath for 12 h.

Synthetic polymer hybrids were prepared similarly. In a typical preparation, 100 mL of 10 wt % aqueous polyvinyl alcohol solution was obtained by dissolving a preweighed amount of PVA in deionized water at 90 $^{\circ}\text{C}$ followed by its mechanical stirring for about 3 h so as to obtain a clear solution. The solution thus obtained was allowed to cool to room temperature. A 2 mL of 25 wt % aqueous glutaraldehyde solution was added to it gradually followed by its mechanical stirring for about 4 h for *in situ* chemical crosslinking with PVA. A required amount of poly (sodium-polystyrene sulfonate) (25 wt % with respect to PVA) dissolved in water was added to the above solution. The admixture was stirred at room temperature till homogeneous slurry was obtained that was casted as a membrane on a smooth flat Plexiglas plate. Removing the solvent and curing the resultant membrane produced a water-insoluble PVA-PSSA hybrid mem-

brane. The membrane was dipped in 3 wt % H₂SO₄ for about 6 h at $\sim 30^{\circ}\text{C}$ to exchange Na⁺ ions in the membrane with protons. The hybrid membrane was subsequently copiously washed with deionized water to expel residual H₂SO₄. The membranes were stored in deionized water for later use. Thickness of all the membranes, as measured by thickness gauge, was $\sim 150\ \mu\text{m}$.

Membrane characterization

Mechanical properties

Universal testing machine (Model AGS-J, Shimadzu, China) with an operating head load of 10 kN was used to study the mechanical properties of the membranes. For the study, cross-sectional area of a membrane sample with known width and thickness was calculated. The test membrane was prepared in the form of dumbbell-shaped object as per ASTM D-882 standards and was placed in the sample holder of the machine. The film was stretched at the crosshead speed of 1 mm/min and its tensile strength was calculated using the equation:

$$\text{Tensile strength (N/mm}^2\text{)} = \frac{\text{Maximum load}}{\text{Cross-sectional area}} \quad (1)$$

A minimum of three measurements were conducted for Nafion-117, CS-HEC-MMT and PVA-PSSA membranes and the average values were taken for their tensile strengths and elongations at break.

Thermal analysis

Thermo gravimetric analysis (TGA) and differential thermal analysis (DTA) of the polymeric hybrids were conducted using SDT Q600 V8.2 TGA/DTA Instrument (USA) in the temperature range between 25 $^{\circ}\text{C}$ and 520 $^{\circ}\text{C}$ at a heating rate of 20 $^{\circ}\text{C}/\text{min}$ with nitrogen flushed at 200 mL/min.

Scanning electron microscopy

Surface micrographs for CS-HEC-MMT and PVA-PSSA polymeric hybrid membranes were obtained using JEOL JSM 35CF scanning electron microscope (SEM). A gold coating of thickness $< 100\ \text{nm}$ was provided on the membrane surface using a JEOL Fine Coat Ion Sputter-JFC-1100 sputtering unit for the SEM study.

Sorption

Sorption experiments were performed gravimetrically on all the membranes in deionized water between 30 $^{\circ}\text{C}$ and 70 $^{\circ}\text{C}$. Initial mass values for the

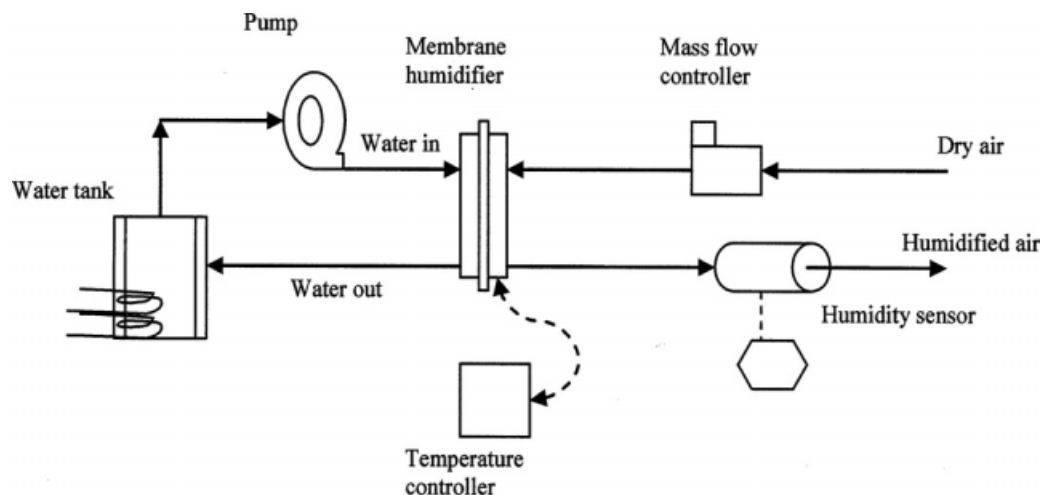


Figure 1 Schematic description of the humidification setup.

circularly cut (diameter = 2.5 cm) CS-HEC-MMT and PVA-PSSA hybrid membranes were obtained by placing them on a single-pan digital microbalance (Sartorius, Germany) sensitive to ± 0.01 mg. Samples saturated in deionized water were transferred to test bottles and kept in a hot air oven maintained at the desired temperature for 48 h. The swollen membranes were weighed soon after surface drying on a digital single-pan microbalance.

The % sorption was calculated from:

$$\% \text{ Sorption} = \left(\frac{W_{\infty} - W_0}{W_0} \right) \times 100 \quad (2)$$

where W_{∞} and W_0 are the weights of sorbed and dry membranes, respectively.

Humidification

The humidification data on polymer hybrid membranes were obtained by sandwiching the sample

membrane between two injection-molded graphite plates with flow channels. To reduce the direct pressure on the membrane materials, a smooth carbon cloth was used on either side of the flow-field plates and the cell was made gas tight. The setup is shown schematically in Figure 1. Dry air was passed on one side of the cell at the flow rates ranging between 1 and 10 standard liters per minute (slpm). Deionized water was fed from the reservoir to the other side of the cell at 20 mL/min. The humidified-air output at different air-flow rate was recorded through a humidification sensor attached to the cell. Mixing ratio and water flux were measured from the humidified-air out flow.

Water flux (J_w) was obtained using the expression:

$$J_w = \left[\frac{X \cdot \rho \cdot Q}{A} \right] \quad (3)$$

where Q is the flowrate of the air (1–10 slpm), ρ is the density of air (1.29 kg/m^3), A is area of the

TABLE I
Mixing Ratio (X) for Different Polymeric Hybrids at Varying Temperatures and Different Air-Flow Rates (Q)

F/R (Q) (SLPM)	Temperature ($^{\circ}\text{C}$)														
	30			40			50			60			70		
	Mixing ratio (X) (g/kg)														
	1	2	3	1	2	3	1	2	3	1	2	3	1	2	3
1	22.4	20.5	22.5	33.1	33.5	–	47.7	47.0	50.1	56.4	70.6	–	86.1	98.1	–
2	19.6	17.8	21.3	31.8	31.7	–	45.4	44.5	49.8	54.7	60.5	–	76.8	80.4	–
3	17.5	15.5	20.2	29.8	27.3	–	42.9	37.7	49.2	49.9	50.9	–	61.1	65.1	–
4	16.1	13.7	19.3	26.4	22.6	–	40.1	30.9	47.3	44.5	41.6	–	54.0	53.5	–
5	14.7	11.9	18.5	24.4	19.5	–	37.8	26.0	45.4	38.9	35.2	–	46.8	44.7	–
6	13.6	10.7	17.6	22.3	16.8	–	33.9	22.3	42.5	34.6	30.2	–	41.6	38.6	–
7	12.7	9.5	16.7	20.7	15.0	–	30.9	19.8	39.9	31.2	26.7	–	36.4	34.0	–
8	11.8	8.8	15.9	19.4	13.6	–	28.7	17.8	37.9	28.7	23.6	–	33.2	30.5	–
9	11.1	8.1	15.2	18.2	12.4	–	26.4	16.2	35.8	26.6	21.7	–	30.5	27.8	–
10	10.5	7.6	14.6	17.5	11.6	–	24.7	15.2	34.1	25.8	20.0	–	28.2	25.8	–

F/R, flow rate; 1, Nafion-117; 2, CS-HEC-MMT; 3, PVA-PSSA.

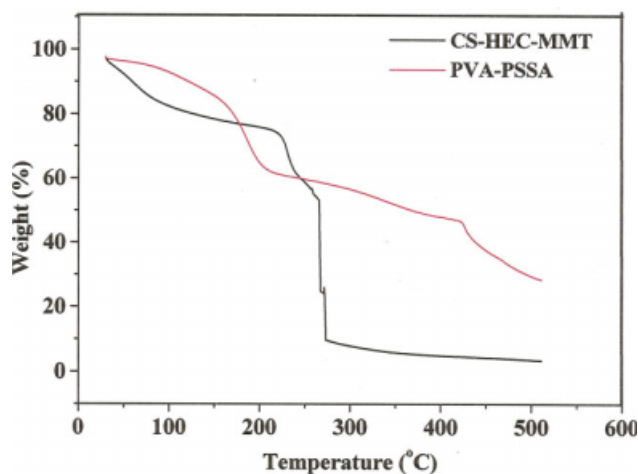


Figure 2 TGA plots for CS-HEC-MMT and PVA-PSSA hybrid membranes. [Color figure can be viewed in the online issue, which is available at www.interscience.wiley.com.]

membrane ($25 \times 10^{-4} \text{ m}^2$), and X is the air/water mixing ratio. All the numerical values of mixing ratios to determine water flux for air humidification at varying temperatures are presented in Table I.

RESULTS AND DISCUSSION

Thermal analysis

Figure 2 illustrates TGA data for CS-HEC-MMT and PVA-PSSA hybrid membranes. With increasing temperature, natural polymeric hybrid CS-HEC-MMT shows different regions of weight loss between 25°C and 520°C characteristic of CS, HEC, and MMT.²⁰ All these constituents lose weight with varying rates at different temperatures. The first weight loss at 221°C is due to the degradation of CS, whereas the

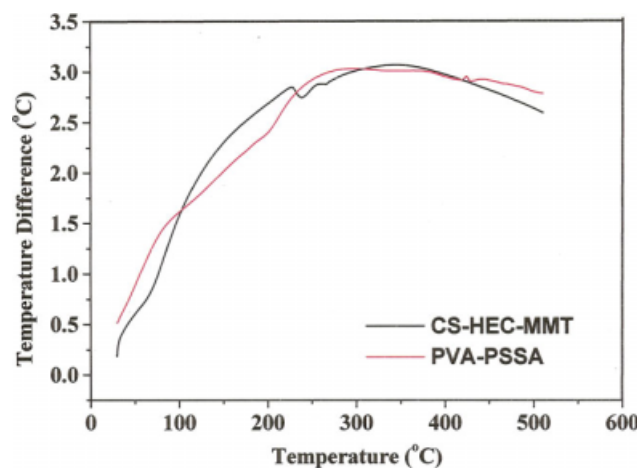


Figure 3 DTA plots for CS-HEC-MMT and PVA-PSSA hybrid membranes. [Color figure can be viewed in the online issue, which is available at www.interscience.wiley.com.]

second loss at 259°C is due to the degradation of HEC. The weight losses at 267°C and 274°C correspond to the decomposition of main chains of CS and HEC. The remnant weight subsequent to the polymer decomposition is due to the residual MMT. Similarly, PVA-PSSA hybrid membranes exhibit three main degradation stages arising due to thermal dehydration, thermal desulfonation, and thermal oxidation of the polymer matrix.²¹ The first weight loss at 152°C is due to the evaporation of surface moisture in the hybrid membranes, whereas the second weight loss at 199°C corresponds to loss of sulfonic acid groups by desulfonation and the third weight loss at 417°C is due to the decomposition of the main chains of the PVA.

Figure 3 represents the DTA thermogram obtained for both the samples in nitrogen, which illustrates two endotherms and one exotherm based on the reaction transition temperatures. The transition region for CS-HEC-MMT lies between 200°C and 350°C, whereas transition region for PVA-PSSA lies between 80°C and 430°C, and corresponds to the net weight loss observed during TGA.

Membrane mechanical stability

Mechanical stability optimization of the membrane is seminal toward its use for humidification. Tensile

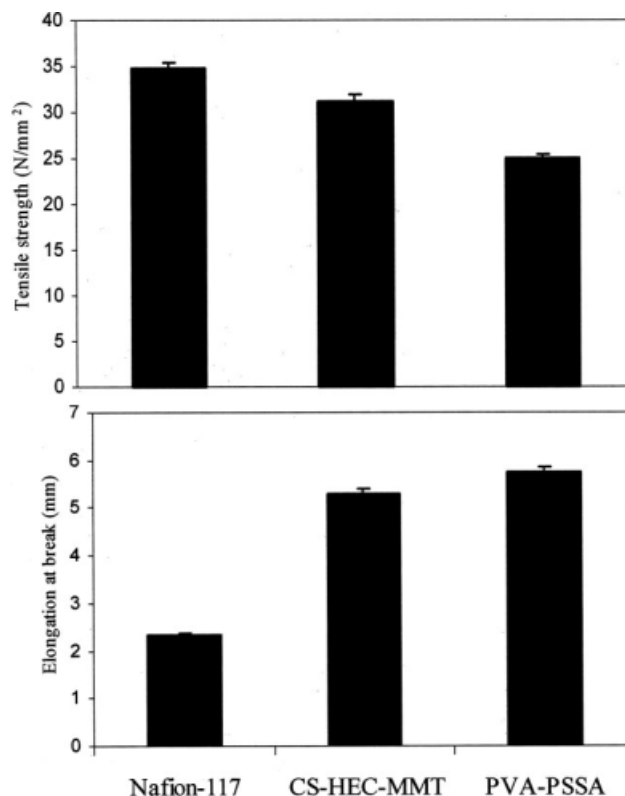
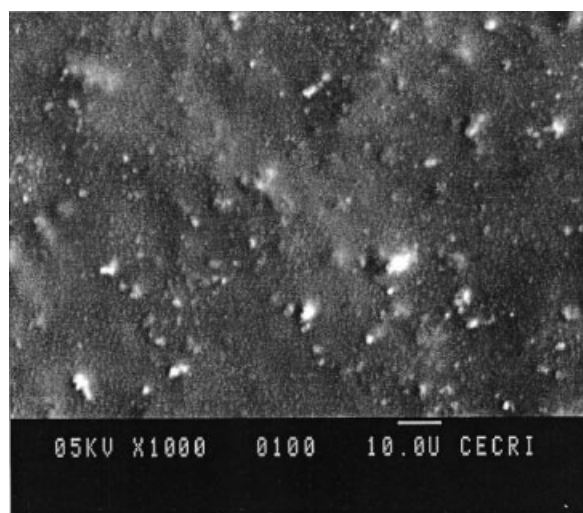
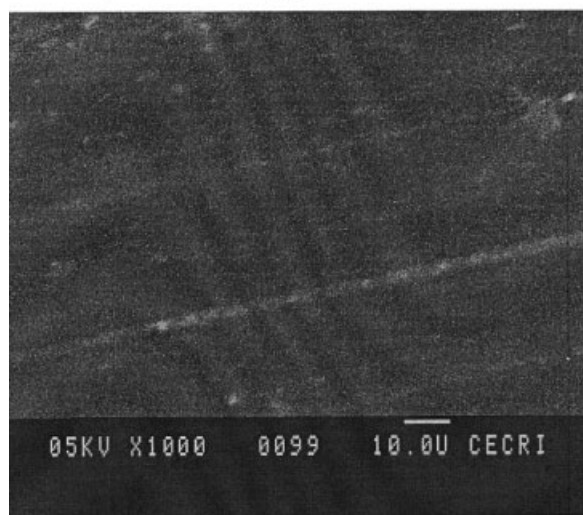


Figure 4 Tensile strength and elongation at break for Nafion[®], CS-HEC-MMT, and PVA-PSSA membranes.



(a)



(b)

Figure 5 Surface scanning electron micrographs for (a) CS-HEC-MMT and (b) PVA-PSSA membranes.

strengths at break for CS-HEC-MMT and PVA-PSSA hybrid membranes are compared with Nafion[®] membrane in dry state in Figure 4. The data suggest that the tensile strength for the membranes vary as: Nafion[®] membrane > CS-HEC-MMT membrane > PVA-PSSA membranes. The higher tensile strength for CS-HEC-MMT membrane than PVA-PSSA membrane is attributed to the interaction of MMT particles with CS-HEC matrix. CS-HEC chains in presence of MMT filler particles experience a restriction in chain segmental mobility increasing rigidity or tensile strength of the membrane with consequent reduction in the elongation at break. PVA-PSSA hybrid membrane minimizes the restriction in chain segmental mobility and renders higher water flux during humidification in relation to CS-HEC-MMT and Nafion[®] membranes albeit at the cost of its mechanical stability.

Membrane morphology

Figure 5(a,b) elucidates the surface SEM micrographs for CS-HEC-MMT and PVA-PSSA membranes. A uniform distribution of MMT particles in the CS-HEC matrix and compatible polymer hybrid of PVA-PSSA matrix is observed from the micrographs. It is noteworthy that uniform dispersion forming a compatible polymer hybrid membrane is desirable for enhanced water flux during humidification.

Sorption

Liquid sorption through polymeric membranes has been well documented in the literature.²² Humidification is influenced by the sorption capacity of membranes. Figure 6 compares the sorption for CS-HEC-MMT and PVA-PSSA hybrid membranes with Nafion[®] membrane at 30, 40, 50, 60, and 70°C. In relation to CS-HEC-MMT, addition of MMT to CS-HEC-MMT restricts the degree of swelling of the membrane in water. Conversely, dual hydrophilic and hydrophobic nature of the Nafion[®] membrane minimizes its swelling. At increased temperatures, sorption increases due to thermal motions of polymer chain segments in response to chain relaxation. For instance, sorption is higher for PVA-PSSA membrane in water at all temperatures due to the higher hydrophilic-hydrophilic interactions in the PVA-PSSA matrix in relation to CS-HEC-MMT and Nafion[®] membranes. Higher sorption causes higher specific interactions, but the extent of interaction between liquid molecules and membrane polymer depends upon the nature of the hybrid used. Figure 7 shows schematic representation of interactions between MMT filler, CS-HEC, and water. The water self-diffusion coefficients for sorption behavior of PVA-PSSA and Nafion[®] membranes as quantified

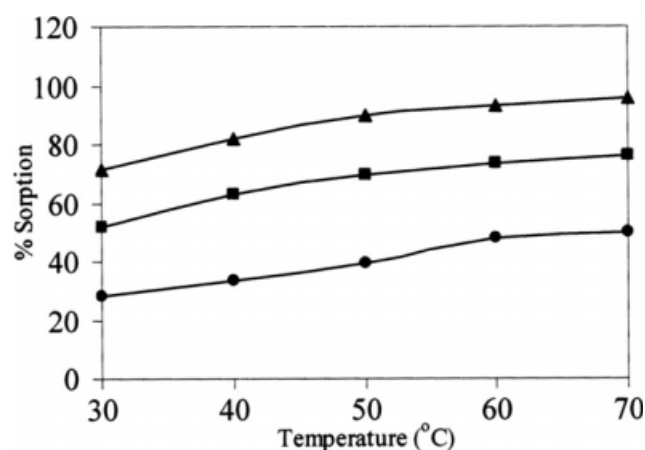


Figure 6 % Sorption vs. temperature. Symbols: (●) Nafion[®]; (■) CS-HEC-MMT, and (▲) PVA-PSSA.

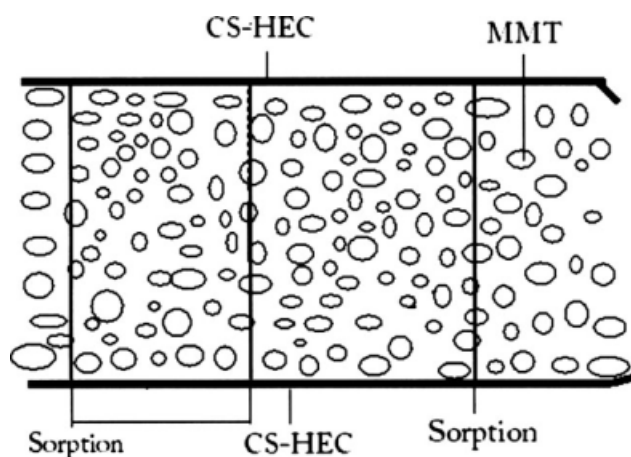


Figure 7 Schematic description of interaction among MMT, CS-HEC, and water.

from NMR imaging technique are $4.87 \times 10^{10} \text{ m}^2/\text{s}$ and $7.53 \times 10^{10} \text{ m}^2/\text{s}$.²³

Performance evaluation

In this study, a portion of the membrane facing each plate in the humidification setup is water permeable facilitating water exchange between liquid and air streams. Relative humidity values for PVA-PSSA membranes vary between 90 and 60% with varying air-flow rates that are higher than the relative humidity values (90–30%) observed for CS-HEC-MMT membranes. By contrast, relative humidity values for Nafion-117 are found to vary between 95 and 80% under identical test conditions in accordance with the literature.¹⁷ Percentage relative humidity and dew point values for all the membranes at varying air-flow rates at 30°C are given in Table II. For all the membranes, the relative humidity and dew point values decrease with increasing flow rate, which could be attributed to the limited rate of water transport through the membrane and water evaporation at the membrane/gas interface.¹² The

amount of water transporting across the membrane and mixing with the air is related to the membrane active area at a given temperature that determines the water flux.

Dual hydrophilic–hydrophilic interaction of the hybrid CS-HEC and MMT particles plays an important role in achieving a high water flux. Figure 8 shows an increase in the water flux for CS-HEC-MMT hybrid membrane with air-flow rates between 1 and 10 slpm with temperatures varying from 30°C to 70°C. Water molecules are absorbed through the voids of the membrane making it water permeable while keeping it gas impermeable which helps in providing an optimum mixing ratio for air output of desired humidity. Water flux for CS-HEC-MMT membrane is lower than Nafion® membrane due to the decrease in the segmental chain mobility of CS-HEC-MMT polymer but its operational stability is comparable to Nafion® membrane.

Our results conform to adsorption–diffusion–desorption principles²⁴ with the conventional observation that humidification takes place due to selective adsorption of water onto MMT clay particles in addition to small defects between neighboring crystal blocks of clay and nonclay pores that will inhibit the transport of air and will prevent inter-mixing. Accordingly, water flux increases as the driving force for permeation increases concomitant to a faster desorption rate on either side. This effect is more favorable for water transport because water molecules occupy most of the free channels in the hydrophilic clay region of the hybrid membranes.²⁵ This also justifies a marked increase in water flux with temperature making hybrid membranes of this study highly water selective.

Both PVA and PSSA are hydrophilic in nature and an increased water flux with temperature is expected. Figure 9 shows the variation of water flux for PVA-PSSA hybrid membrane at 30°C and 50°C. PVA-PSSA hybrid membrane exhibits a higher water flux in relation to Nafion® membrane because the

TABLE II
% Relative Humidity and Dew Point (°C) for Different Air-Flow Rates (Q) at 30°C

F/R (Q) (SLPM)	Nafion-117		CS-HEC-MMT		PVA-PSSA	
	Dew point (°C)	% RH	Dew point (°C)	% RH	Dew point (°C)	% RH
1	26.7	95	25.3	86	26.8	89
2	24.6	93	23.0	76	25.9	85
3	22.7	91	20.7	67	25.1	81
4	21.4	89	18.9	60	24.3	78
5	20.0	87	16.6	53	23.6	75
6	18.8	84	14.9	48	22.8	72
7	17.6	83	13.3	44	22.0	69
8	16.5	82	11.9	43	21.3	66
9	15.6	81	10.8	39	20.5	64
10	14.8	80	10.0	36	19.9	61

former has better water uptake capacity. Our earlier study on proton conductivity and water uptake capacity of PVA-PSSA membrane suggests it to be compatible for application in PEFCs.²⁶ However, PVA-PSSA hybrid membrane shows poor operational stability above 50°C due to the thermal agitation of the polymer chains leading to a higher degree of swelling that may cause membrane rupturing during humidification. Accordingly, the present study has been restricted to 50°C. It is noteworthy that water flux for PVA-PSSA membrane is higher than Nafion[®] membrane because hydrophilic groups in the former absorb water more preferentially than the latter.

CONCLUSIONS

The study demonstrates the utility of synthetic and natural polymeric hybrid membranes for air humidification in PEFCs. Humidified-air outputs from the humidifier using aforesaid membranes are comparable with the humidifier using commercial Nafion[®]

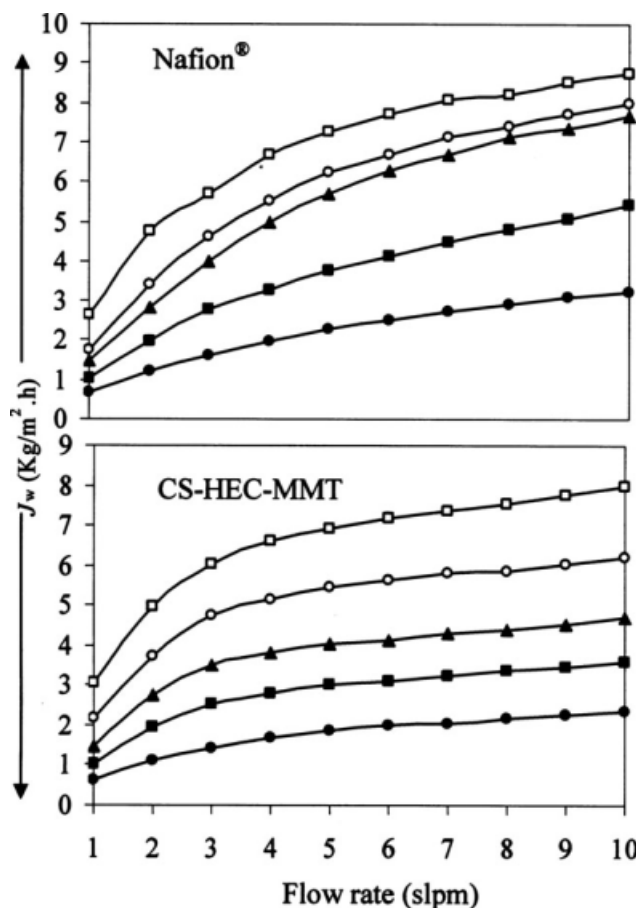


Figure 8 Water flux vs. air-flow rate (1–10 slpm) for Nafion[®] and CS-HEC-MMT membranes at varying temperatures. Symbols: (●) 30°C; (■) 40°C; (▲) 50°C; (○) 60°C; and (□) 70°C.

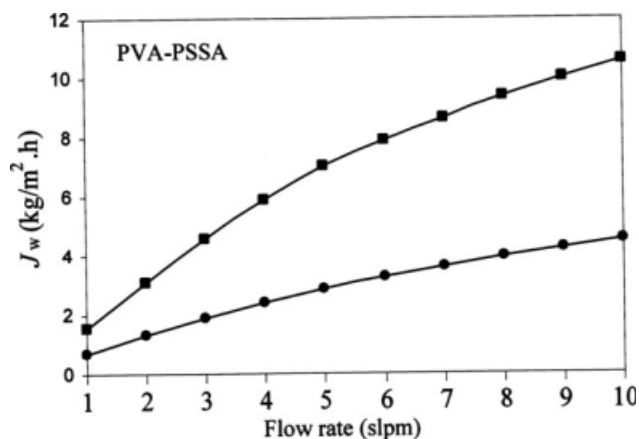


Figure 9 Water flux vs. air-flow rate (1–10 slpm) for PVA-PSSA membranes at different temperatures. Symbols: (●) 30°C and (■) 50°C.

membrane. Equilibrium sorption data demonstrate an attractive water uptake capacity for PVA-PSSA hybrid membrane, but it has poor operational stability above 50°C. CS-HEC-MMT membrane has dual hydrophilic–hydrophilic interaction and the incorporation of MMT fillers in this membrane helps providing high sorption capacity with increased water flux. The two hybrid polymeric membranes reported here are cost-effective and, hence, can be widely used for air humidification. However, striking a balance between water flux and operational stability of these membranes is desired for application in PEFCs.

References

- Kang, M. S.; Kim, J. H.; Won, J.; Moon, S. H.; Kang, Y. S. *J Membr Sci* 2005, 247, 127.
- Cui, Z.; Liu, C.; Lu, T.; Xing, W. *J Power Sources* 2007, 167, 94.
- Yamada, M.; Honma, I. *Electrochim Acta* 2005, 50, 2837.
- Lin, C. W.; Huang, Y. F.; Kannan, A. M. *J Power Sources* 2007, 164, 449.
- Jung, S. H.; Kim, S. L.; Kim, M. S.; Park, Y.; Lim, T. W. *J Power Sources* 2007, 170, 324.
- Sun, H.; Zhang, G.; Guo, L. J.; Dehua, S.; Liu, H. *J Power Sources* 2007, 168, 400.
- Sridhar, P.; Perumal, R.; Rajalakshmi, N.; Raja, M.; Dhathathreyan, K. S. *J Power Sources* 2001, 101, 72.
- Guvelioglu, G. H.; Stenger, H. G. *J Power Sources* 2007, 163, 882.
- Mossman, A. D. U.S. Pat. 6,864,005 B2 (2005).
- Voss, H. H.; Barton, R. H.; Wells, B. W.; Ronne, J. A.; Nigsch, H. A. U.S. Pat. 6,416,895 B1 (2002).
- Murphy, O. J.; Hitchens, G. D.; Cisar, A. J.; Martin, A. G. U.S. Pat. 5,996,976 (1999).
- Mazzucchelli, G.; Brambilla, M.; Fleba, G. P.; Maggiore, A. U.S. Pat. 6,737,183 B1 (2004).
- Hyun, D.; Kim, J. *J Power Sources* 2004, 126, 98.
- Yan, Q.; Toghiani, H.; Wu, J. *J Power Sources* 2006, 158, 316.
- Um, S.; Wang, C. H. *J Power Sources* 2006, 156, 211.
- Choi, K. H.; Park, D. J.; Rho, Y. W.; Kho, Y. T.; Lee, T. H. *J Power Sources* 1998, 74, 146.

17. Park, S. K.; Cho, E. A.; Oh, I. H. *Korean J Chem Eng* 2005, 22, 877.
18. Shao, P.; Huang, R. Y. M. *J Membr Sci* 2007, 287, 162.
19. Wijmans, J. G.; Baker, R. W. *J Membr Sci* 1995, 107, 1.
20. Kanti, P.; Srigowari, K.; Madhuri, J.; Smitha, B.; Sridhar, S. *Sep Purif Technol* 2004, 40, 259.
21. Holland, B. J.; Hay, J. N. *Polymer* 2001, 42, 6775.
22. Crank, J. *The Mathematics of Diffusion*; Clarendon Press: Oxford, UK, 1975.
23. Sahu, A. K.; Selvarani, G.; Bhat, S. D.; Pitchumani, S.; Sridhar, P.; Shukla, A. K.; Narayanan, N.; Banerjee, A.; Chandrakumar, N. *J Membr Sci* 2008, 319, 298.
24. Feng, X.; Huang, R. Y. M. *Ind Eng Chem Res* 1997, 36, 1048.
25. Bhat, S. D.; Aminabhavi, T. M. *Sep Purif Technol* 2006, 51, 85.
26. Sahu, A. K.; Selvarani, G.; Pitchumani, S.; Sridhar, P.; Shukla, A. K.; Narayanan, N.; Banerjee, A.; Chandrakumar, N. *J Electrochem Soc* 2008, 155, B686.